Principles of ligand binding within a completely buried cavity in HIF2α PAS-B

Supporting Information

Jason Key, Thomas H. Scheuermann, Peter C. Anderson, Valerie Daggett and Kevin H. Gardner

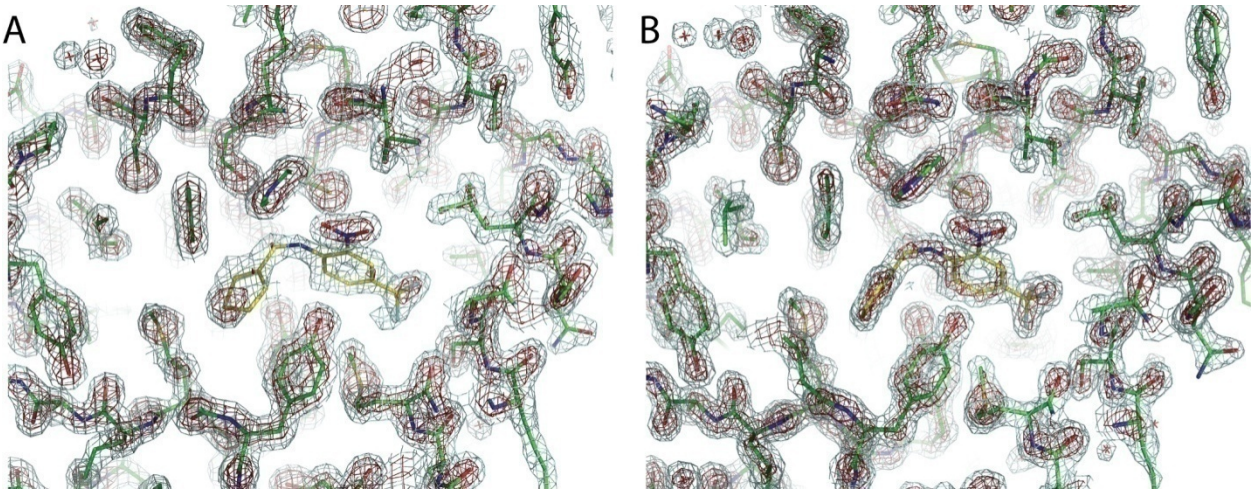

SI Figure 1. Electron density of HIF2α PAS-B subunit of the ARNT/HIF2α PAS-B heterodimer with bound ligand.(A). The $2F_o$-F_c electron density map for THS-020 structure **(B)**.The $2F_o$-F_c electron density for THS-017 structure. Ligands are shown in yellow atoms at the center of each panel. Density is contoured at 1.5 (cyan) and 3 (red) sigma where sigma represents the R.M.S deviation across the asymmetric unit.

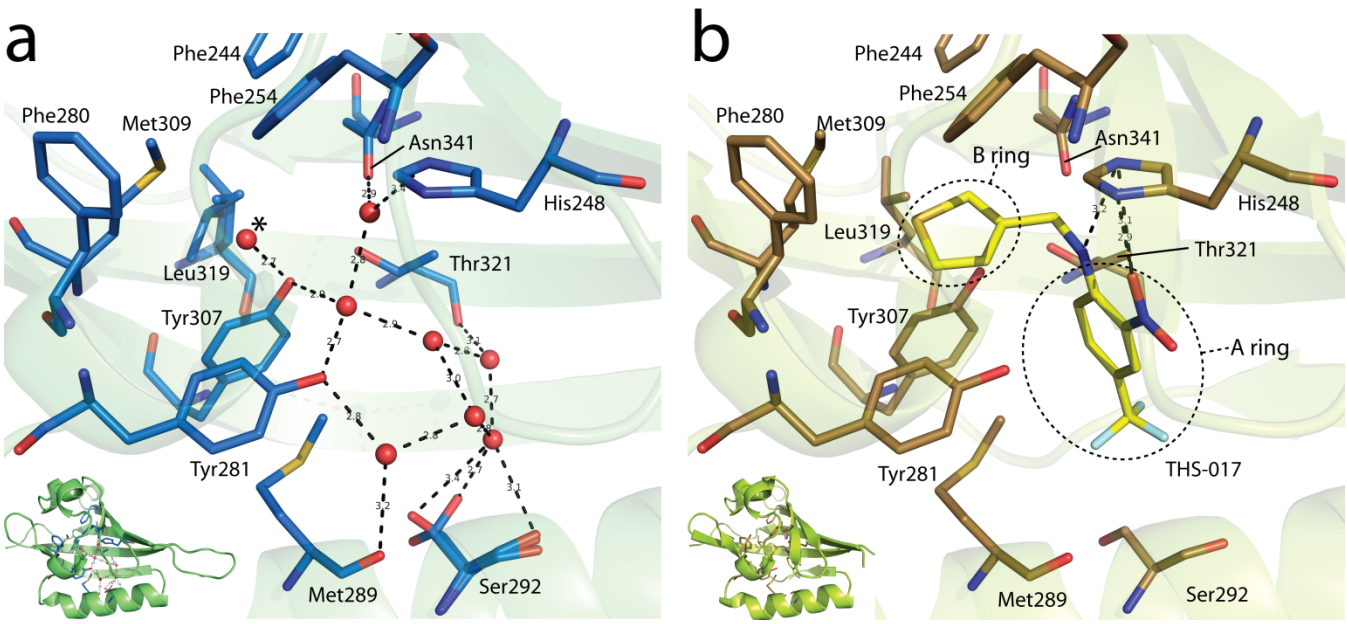

SI Figure 2. Electron density of HIF2α PAS-B subunit of the ARNT/HIF2α PAS-B heterodimer with bound ligand.(A). Hydrogen bonds in the water-bound unliganded form of HIF2α PAS-B[1] (PDB code 3F1P). **(B)**. Hydrogen bonds in the HIF2α PAS-B bound to the compound THS-017 (PDB code 3H7W). Orientation of the molecule is show in the lower right as a ribbon diagram. The water molecule observed in the predominantly hydrophobic end of the cavity is noted with an asterisk (*).

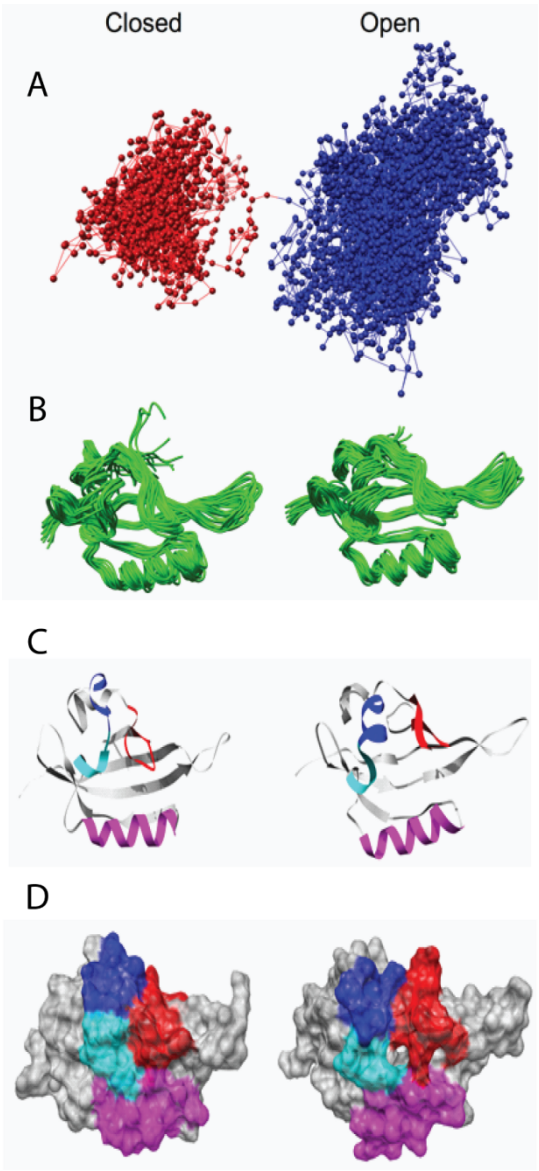

SI Figure 3. HIF2α PAS-B conformations.(A). Projection of all-versus-all comparison of Cα RMSDs for all structures over simulation 1. The dimensionality of the matrix is then reduced to yield a project that approximates the actual RMSDs between structures. The points are connected by time and begin in the closed state (red). Over time, the protein converts to the open state (blue). When points cluster together in the projection they are necessarily similar. The projection displayed is for run 1, conversion to the open state and back was observed in the other two simulations. **(B)**. Many structures from the different conformational ensembles are displayed below the projection to illustrate both the dynamic nature of the structures, particularly the helices and loops, and the differences between the conformers. The average Cα RMSD between the two conformational states is 3.6 Å. **(C)**. Representative structures from run 1 are displayed. The structure on the left is closed and at 0 ns of MD. The 16 ns open structure is shown to the right. In both cases Dα (blue), Eα (cyan), Fα (magenta), and the AB hairpin and loop (red) are highlighted. **(D)**. Space filling versions of the structures in panel C (rotated slightly) are displayed; note the channel above Fα due to the movement of the helices.

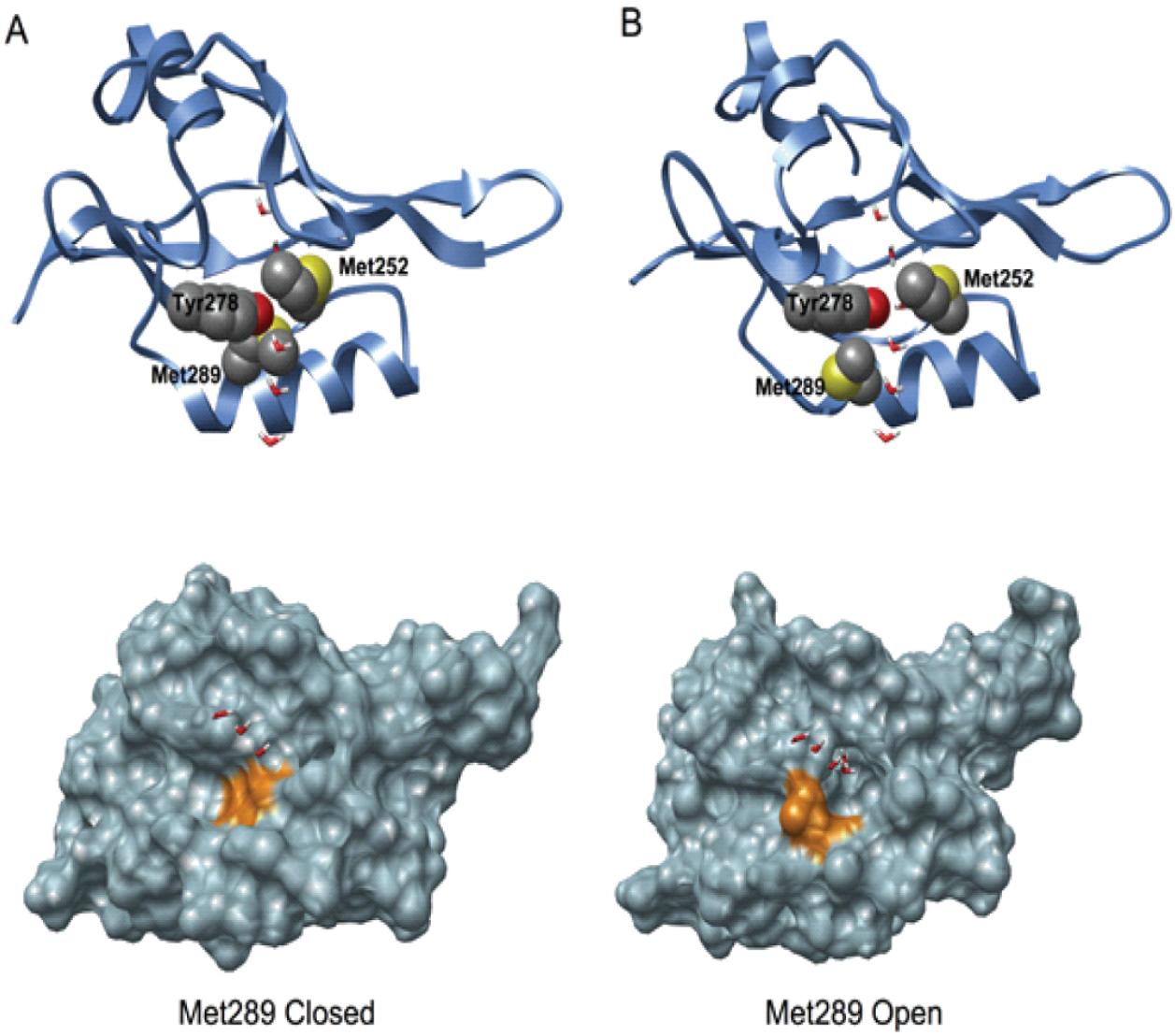

SI Figure 4. Met 289 side chain conformational change allows water passage between AB-loop, Eα and Fα when HIF2α PAS-B is in closed conformation. Met 289 exists in different rotameric states in the MD simulations. **(A)**. When in a closed conformation, the Met289 side chain blocks the passage along with the Met 252 and Tyr 278 side chains. **(B)**. An open conformation of Met 289 opens the passage. The corresponding surface representation of the protein is displayed with Met 289 highlighted in orange and the protein rotated to best show the Met 289 gating.

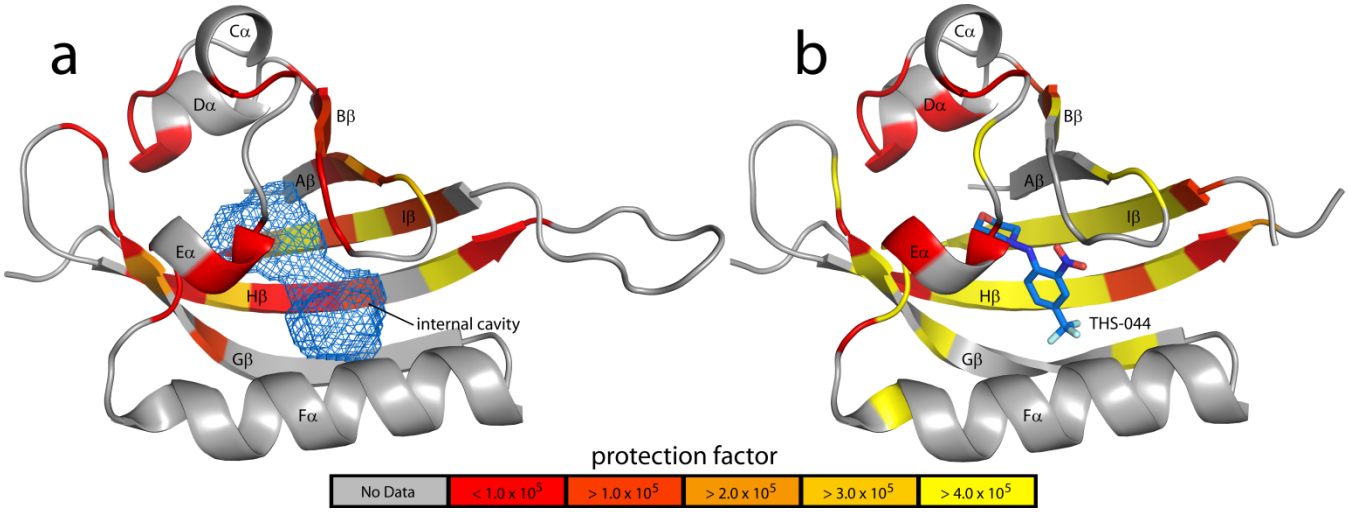

SI Figure 5. Deuterium exchange protection factors for the unliganded and ligand-bound forms of HIF2α PAS-B mapped onto the unbound (a) and liganded (b) crystal structures[1] (PDB codes 3F1P, 3F1O respectively). Regions mapped in grey indicate backbone amide probes which exchange within the time of the first measurement (approximately 20 minutes). Data was obtained at pH 6.8 (uncorrected in D_2O) and 25°C.[1]

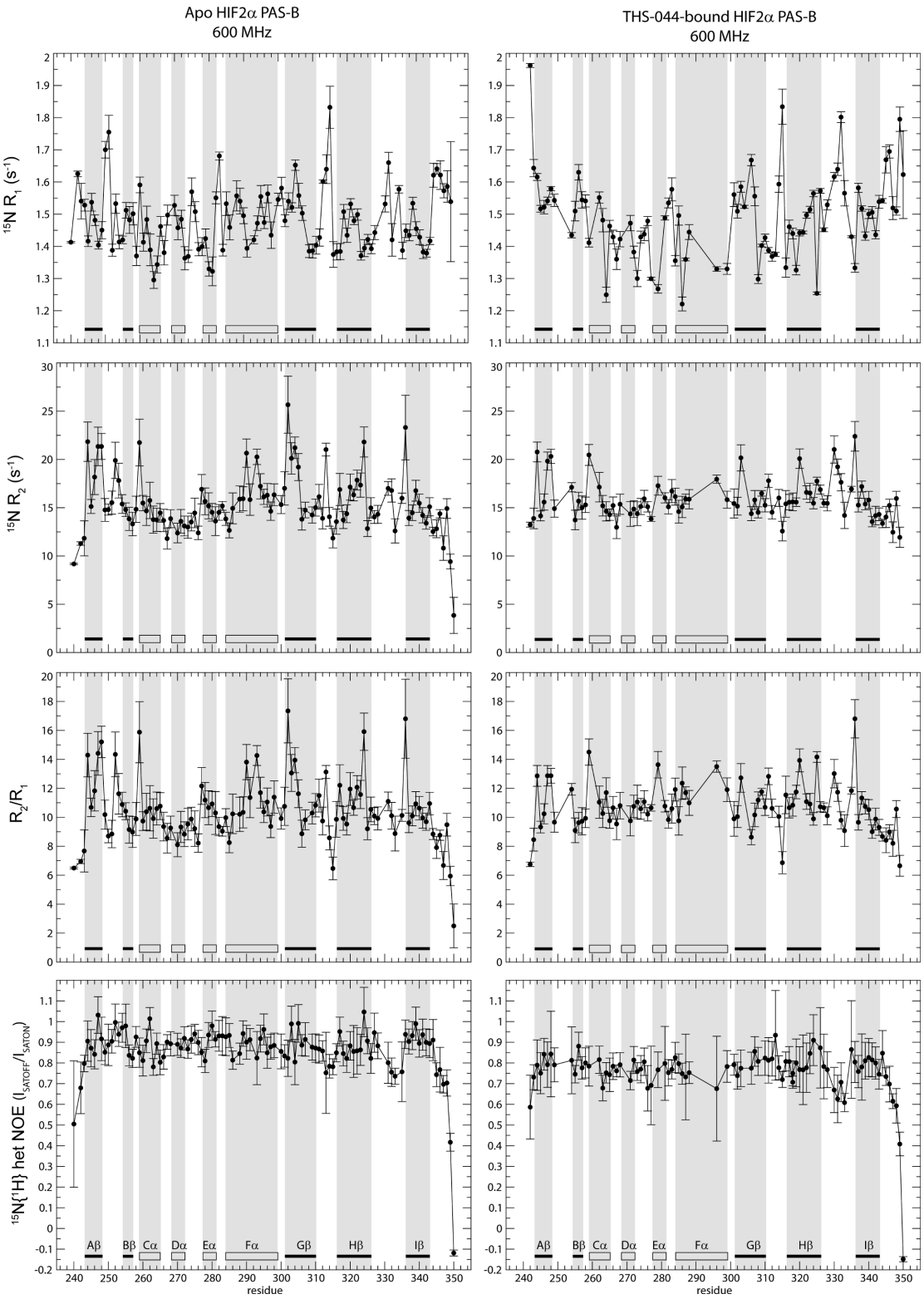

SI Figure 6. ^{15}N relaxation measurements from HIF2α PAS-B in the absence of presence of an artificial ligand, compound THS-044. Shown are ^{15}N R_1, R_2, R_1/R_2 relaxation rates (from single exponential fits) and ^{15}N{^{1}H} NOE values.

$$dMz_{aa}/dt = k_{ba}\, Mz_{ab} - Mz_{aa}\,(k_{ab} + R1_a)$$

$$dMz_{bb}/dt = k_{ab}\, Mz_{ba} - Mz_{bb}\,(k_{ba} + R1_b)$$

$$dMz_{ab}/dt = k_{ab}\, Mz_{aa} - Mz_{ab}\,(k_{ba} + R1_b)$$

$$dMz_{ba}/dt = k_{ba}\, Mz_{bb} - Mz_{ba}\,(k_{ab} + R1_a)$$

SI Figure 7. The McConnell equations[2,3] used to fit time-dependent peak intensity for NMR ZZ-exchange for a system under two-state exchange from state a to state b. Mz denotes magnetization along the longitudinal(z) axis, k is the exchange rate constant, and R1 is the ^{15}N longitudinal relaxation rate. The subscripts for Mz (aa, bb, ab, and ba) indicate autopeaks (aa, bb) and cross-peaks (ab, ba) for the unbound (a) and bound (b) states. In the case of rate constants, the subscripts indicate exchange from unbound to bound (ab), or from bound to unbound states (ba).

Event #	Time (ns)	Entry or Egress	Route (See Fig. 5)	Protein Conformation (see SI Fig. 1)	M289 rotomer (See SI Fig. 2)	Simulation Run (of 3 total)
1	0.4	Egress	2	Closed	Open	1
2	0.6	Egress	2	Closed	Open	1
3	0.6	Egress	2	Closed	Open	1
4	1.2	Egress	2	Closed	Open	1
5	4.5	Egress	3	Closed	Open	1
6	7.0	Egress	2	Closed	Open	1
7	8.1	Entry	3	Closed	Open	1
8	14.6	Entry	2	Open	Open	1
9	15.0	Egress	2	Open	Open	1
10	16.6	Egress	2	Open	Open	1
11	21.2	Entry	2	Open	Open	1
12	22.1	Entry	2	Open	Open	1
13	22.3	Egress	2	Open	Closed	1
14	23.3	Entry	2	Open	Open	1
15	25.3	Egress	2	Open	Closed	1
16	27.2	Egress	2	Open	Closed	1
17	32.4	Entry	1	Open	Closed	1
18	32.5	Entry	2	Open	Closed	1
19	32.6	Entry	1	Open	Closed	1
20	32.9	Entry	1	Open	Closed	1
21	33.2	Egress	1	Open	Closed	1
22	33.6	Egress	2	Open	Closed	1
23	34.0	Egress	1	Open	Closed	1
24	34.7	Egress	1	Open	Closed	1
25	2.0	Entry	1	Open	Open	2
26	2.1	Egress	2	Open	Open	2
27	2.2	Egress	2	Open	Open	2
28	2.2	Egress	2	Open	Open	2

29	2.3	Egress	2	Open	Open	2
30	2.3	Egress	1	Open	Open	2
31	6.9	Entry	1	Open	Closed	2
32	7.2	Egress	2	Open	Closed	2
33	1.0	Egress	1	Open	Open	3
34	1.5	Egress	1	Open	Open	3
35	2.0	Entry	1	Open	Open	3
36	2.9	Entry	1	Open	Open	3
37	3.0	Entry	1	Open	Open	3
38	3.1	Egress	1	Open	Open	3
39	3.1	Entry	1	Open	Open	3
40	3.3	Egress	1	Open	Open	3
41	3.5	Egress	1	Open	Open	3
42	3.7	Entry	1	Open	Open	3
43	4.5	Egress	1	Open	Open	3
44	4.9	Egress	1	Open	Open	3
45	4.9	Egress	1	Open	Open	3
46	7.0	Egress	1	Open	Open	3

Supplementary Table 1. Water passage in the Hif2α PAS-B MD simulations. The time for water passage is given for each event in each of the three simulations. Note that water is placed in the cavity during the preparatory solvation steps for, but prior to, MD. Direction of transfer, conformation (open or closed), route (see Fig. 5), and the disposition of Met 289 are indicated.

Supporting Information References

1. Scheuermann, T. H.; Tomchick, D. R.; Machius, M.; Guo, Y.; Bruick, R. K.; Gardner, K. H., Artificial ligand binding within the HIF2alpha PAS-B domain of the HIF2 transcription factor. *Proc Natl Acad Sci U S A* **2009,** 106, (2), 450-5.
2. Farrow, N. A.; Zhang, O.; Forman-Kay, J. D.; Kay, L. E., A heteronuclear correlation experiment for simultaneous determination of 15N longitudinal decay and chemical exchange rates of systems in slow equilibrium. *J Biomol NMR* **1994,** 4, (5), 727-34.
3. Iwahara, J.; Clore, G. M., Direct observation of enhanced translocation of a homeodomain between DNA cognate sites by NMR exchange spectroscopy. *J Am Chem Soc* **2006,** 128, (2), 404-5.